Journal of King Saud University - Science 36 (2024) 103307

HOSTED BY

Contents lists available at ScienceDirect

Journal of King Saud University - Science

journal homepage: www.sciencedirect.com

Full Length Article

A novel BSA-coated nano selenium-impregnated scaffold showed improved strength, cellular attachment and proliferation in C2C12 cell

Suresh Naveenkumar [a], Johnson Retnaraj Samuel Selvan Christyraj [b], K. Kaviyarasu [c], Azhaguchamy Muthukumaran [a,*]

[a] Department of Biotechnology, Kalasalingam Academy of Research and Education, Krishnankoil, Tamilnadu, India
[b] Regeneration and Stem Cell Biology Lab, Centre for Molecular and Nanomedical Sciences, International Research Centre, Sathyabama Institute of Science and Technology, Chennai 600119, Tamil Nadu, India
[c] UNESCO-UNISA Africa Chair in Nanoscience's/Nanotechnology Laboratories, College of Graduate Studies, University of South Africa (UNISA), Muckleneuk Ridge, PO Box 392, Pretoria, South Africa

ARTICLE INFO

Keywords:
Antioxidant
Thermal stability
Cellular attachment
Proliferation and C2C12 cell line

ABSTRACT

This study aims to develop scaffolds (CCS, CCS-SeNPs, CCS-SA-SeNPs, and CCS-PET-SeNPs) with enhanced mechanical strength, thermal stability, and antioxidant properties to improve cell attachment and proliferation of the C2C12 cell line for cardiac health applications. Collagen and chitosan are popular biopolymers in tissue engineering for their biocompatibility, biodegradability, and support for cell growth. Selenium nanoparticles (SeNPs) are incorporated into scaffolds for their antioxidant, anti-inflammatory, and antimicrobial properties, which enhance tissue regeneration. Sodium alginate and pectin, natural polysaccharides, further modify these scaffolds to improve structural and functional properties. Developing these composite scaffolds aims to optimize biomaterial performance in regenerative medicine. In the present study, various types of scaffolds (CCS, CCS-SeNPs, CCS-SA-SeNPs, and CCS-PET-SeNPs scaffolds) were prepared and characterized using X-ray diffraction (XRD), Scanning Electron Microscopy with Energy Dispersive X-ray Spectroscopy (SEM-EDX), and Thermo-Gravimetric Analysis (TGA). The XRD data revealed that all the scaffolds (CCS, CCS-SeNPs, CCS-SA-SeNPs, and CCS-PET-SeNPs) displayed an amorphous structure. SEM analysis demonstrated that the CCS and CCS-SA-SeNPs scaffolds exhibit solid-walled metrics and a smooth surface. EDX confirmed the homogeneous Se distribution within the scaffolds. The tensile strength of CCS, CCS-SeNPs, CCS-SA-SeNPs, and CCS-PET-SeNPs scaffolds was found to be 5.15 N, 4.77 N, 4.05 N, and 4.01 N, respectively. Thermal stability assessments showed that CCS-SeNPs, CCS-SA-SeNPs and CCS-PET-SeNPs scaffolds displayed good thermal stability, with maximum decomposition occurring at 250 °C. Furthermore, the CCS-SeNPs, CCS-SA-SeNPs, and CCS-PET-SeNPs scaffolds showed notable antioxidant activity of ~ 57 %, compared to the CCS scaffold's 42 %. Morphological studies of C2C12 cells on these scaffolds showed better proliferation on SeNPs-enhanced scaffolds. Nucleus morphology remained unchanged, indicating no adverse effects from SeNPs. The results indicate that the scaffolds (CCS, CCS-SeNPs, CCS-SA-SeNPs, and CCS-PET-SeNPs) demonstrate notable enhancements in mechanical strength, thermal stability, and antioxidant efficacy. These advancements are anticipated to promote enhanced cell adhesion and proliferation of the C2C12 cell line, thereby emphasizing their potential utility in cardiac health applications.

1. Introduction

In recent years, tissue engineering has emerged as a promising field aiming to regenerate or replace damaged tissues and organs (Han et al., 2023). Success in tissue engineering relies on designing and fabricating biomimetic scaffolds that can provide mechanical support, promote cell adhesion and proliferation, and guide tissue regeneration (Chan and Leong, 2008). Natural polymers such as collagen and chitosan have gained considerable attention in scaffold development due to their biocompatibility, biodegradability, and resemblance to the extracellular matrix (ECM) components found in native tissues (Reddy et al., 2021). Collagen, the most abundant protein in mammals, is critical in maintaining tissue structure and function. Its biocompatibility and cell-adhesive properties make it an ideal candidate for scaffold materials

* Corresponding author.
E-mail address: a.muthukumaran@klu.ac.in (A. Muthukumaran).

https://doi.org/10.1016/j.jksus.2024.103307
Received 22 November 2023; Received in revised form 10 June 2024; Accepted 12 June 2024
Available online 14 June 2024

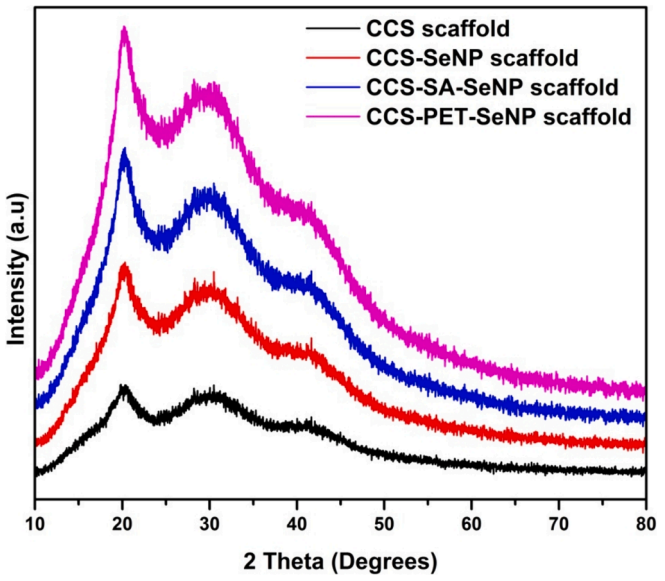

Fig. 1. The XRD patterns illustrate the semi-crystalline nature and phases in the CCS scaffold, CCS-SeNPs, CCS-SA-SeNPs scaffold and CCS-PET-SeNPs scaffold.

(Li et al., 2021). However, collagen scaffolds often lack the mechanical strength and stability required for some tissue engineering applications. Chitosan, derived from chitin, a naturally occurring polysaccharide, possesses intrinsic antibacterial properties, biodegradability, and favorable mechanical characteristics (Islam et al., 2020). The combination of collagen and chitosan has the potential to create scaffolds that synergize the advantages of both materials, resulting in improved structural integrity, enhanced cellular interactions, and overall better performance in tissue regeneration (Zheng et al., 2021). Epidemiological studies have linked selenium deficiency to an increased risk of several diseases, including certain types of cardiovascular disease and thyroid disorders (Naveenkumar et al., 2022). Conversely, selenium supplementation may have protective effects against genotoxicity (Erkekoğlu et al., 2010). However, the relationship between selenium status and disease risk is complex and varies depending on several factors, such as age, sex, and overall health status ((NIH), 2019). Selenium (Se) has been shown to protect against oxidative damage in various organs, including the heart (Sidhu et al., 1993).

Furthermore, previous research has demonstrated that selenium deficiency can lead to oxidative stress and subsequent myocardial injury by activating inflammation, apoptosis, and necroptosis (Lei et al., 2023). These findings underscore the crucial role of selenium in preserving cardiac health by protecting against oxidative stress and supporting antioxidant mechanisms. Nevertheless, selenium deficiency remains widespread in China and many other countries. Various dietary supplements containing selenium, such as sodium selenite, sodium selenate, and selenomethionine, have been developed (Ramoutar and Brumaghim, 2010). The development of selenium-based nanomaterial, including selenium nanoparticles and selenium nanocomposites, explores various synthesis methods and their biomedical applications. These materials have potential as antimicrobial, anticancer, antidiabetic, and antioxidative agents. The study also examines cost-effective and eco-friendly approaches for assessing nano-selenium toxicity *in vitro* and *in vivo* (Sowmya et al., 2024). The quorum quenching activity (QQ) was evaluated in *Pseudomonas aeruginosa* showing in significant reduction in gene expression and virulence factor production across all CS–SeNC dosages as well as biocompatibility tests in a zebrafish model indicated no adverse effects (Karthick Raja Namasivayam et al., 2022). Additionally, biocompatibility tests with human keratinocytes confirmed the nanocomposite's safety, showing no toxicity and indicating its potential antimicrobial agent for modern biomedicine (Namasivayam et al., 2023).

The innovation of this work lies in the comprehensive exploration of functional scaffolds that exhibit exceptional mechanical, thermal, and antioxidant properties, coupled with improved cellular attachment and proliferation. The present study explores different collagen-chitosan scaffolds with selenium nanoparticles, their morphology, mechanical strength, thermal stability and compatibility with the C2C12 cell line.

2. Materials and method

2.1. Synthesis of SeNPs, SA-SeNPs and PET-SeNPs

Selenium nanoparticles were synthesized using a method described by (Naveenkumar et al., 2023). Sodium alginate (100 mg) was dissolved in 100 ml of distilled water and stirred for an hour. This mixture was combined with 0.2 g sodium selenite and 0.3 g ascorbic acid. The above procedure used Pectin for SeNPs preparation (Naveenkumar et al., 2024).

2.2. Preparation of CCS, CCS-SeNPs, CCS-SA-SeNPs and CCS-PET-SeNPs scaffolds

Collagen-Chitosan (CCS) scaffold, Collagen-Chitosan-Selenium nanoparticlev(CCS-SeNPs) scaffold, Collagen-Chitosan-sodium alginate decorated-Selenium nanoparticle (CCS-SA-SeNPs) scaffold and Collagen-Chitosan-pectin decorated-Selenium nanoparticle (CCS-PET-SeNPs) scaffold. Chitosan (1.5 %) was dissolved in distilled water and stirred for 1 h. To this solution, ~15 % of glycerol, 1 ml of SeNPs (10 μg/ml) and 1 % of collagen were added and stirred. The mixture was instantly transferred onto a petri plate and dried for 24 hrs. Afterward, scaffolds were frozen at −80 °C overnight and neutralized with ~ 5 % NaOH for 45 min. Finally, the scaffolds were washed with deionized water and air-dried. The same procedure was followed for preparing the scaffolds with CCS-SA-SeNPs and CCS-PET-SeNPs.

2.3. Characterization of scaffolds

2.3.1. XRD analysis

The XRD analysis was performed to determine the crystalline or amorphous nature of the CCS, CCS-SeNPs, CCS-SA-SeNPs, and CCS-PET-SeNPs scaffolds using a D8 Advance ECO Bruker instrument (Madison, WI, USA). The scanning rate during the XRD measurement was set at 2° per minute.

2.3.2. SEM-EDX analysis

The morphological features of the CCS, CCS-SeNPs, CCS-SA-SeNPs and CCS-PET-SeNPs scaffolds were examined using a SEM (Carl Zeiss, Model EVO 18, Germany). The elemental composition of selected areas of the scaffolds was analyzed in energy-dispersive X-ray spectroscopy (EDAX APEX).

2.3.3. Tensile strength analysis

The tensile strength of the CCS, CCS-SeNPs, CCS-SA-SeNPs and CCS-PET-SeNPs scaffolds were analysis to texture analyzer (Tex Pro-TA10) (Naveenkumar et al., 2023).

2.3.4. Thermal stability analysis

The thermal stability of the CCS, CCS-SeNPs, CCS-SA-SeNPs, and CCS-PET-SeNPs scaffolds was evaluated using a Thermogravimetric analyzer (TGA) (STA 800 Simultaneous Thermal Analyzer, Perkin Elmer).

2.4. Antioxidant activity (DPPH assay)

The method used to assess the antioxidant activity of the CCS, CCS-SeNPs, CCS-SA-SeNPs and CCS-PET-SeNPs scaffolds had been previously

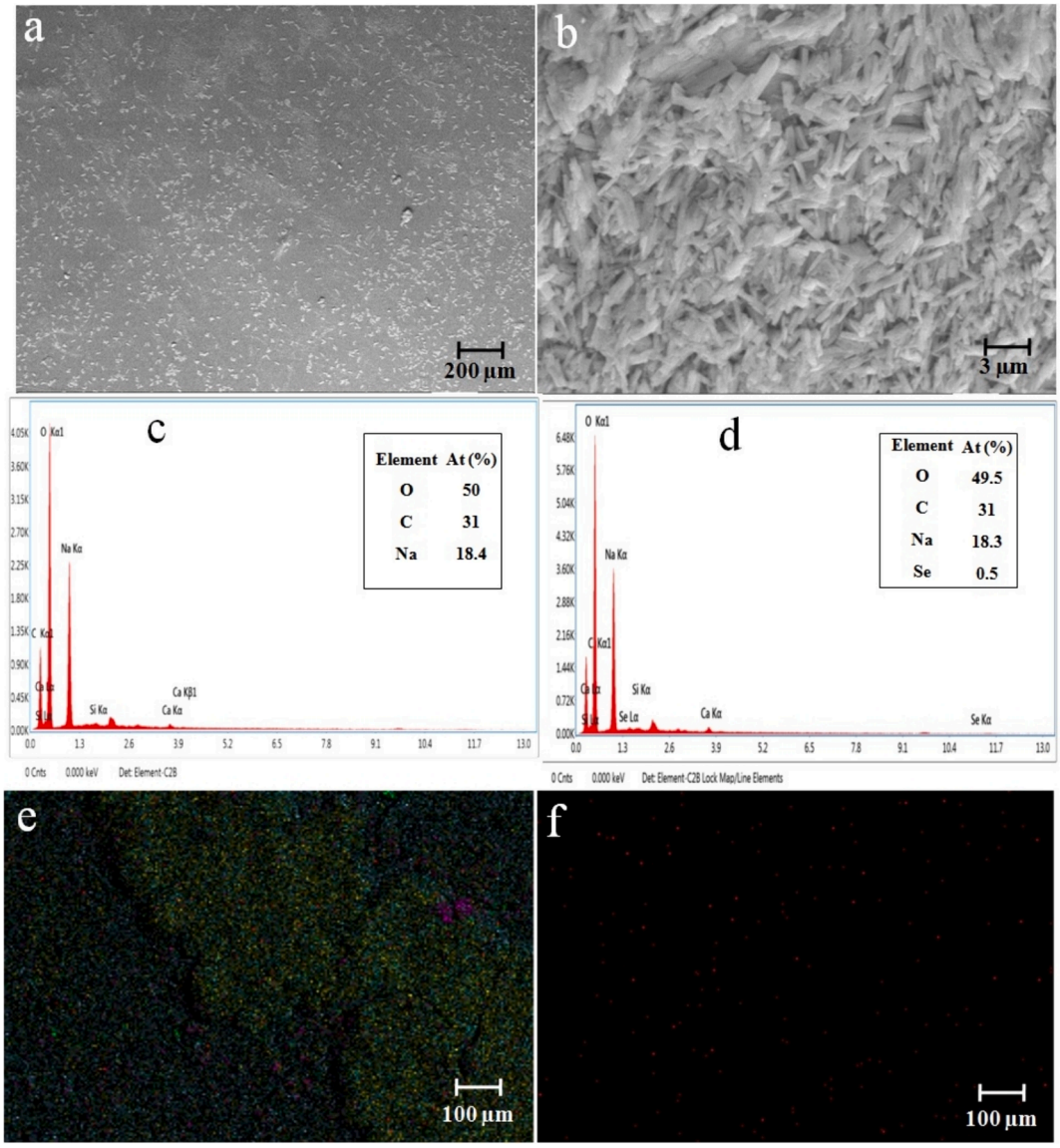

Fig. 2. (a-b) SEM observation of CCS and CCS-SeNPs scaffolds; (c) EDX spectrum and (e) EDX mapping of CCS scaffold; (d) EDX spectrum and (f) EDX mapping of CCS-SeNPs scaffold.

described by Naveenkumar et al. (Naveenkumar et al., 2023).

2.5. Preparation for in vitro tests

In the present study, the scaffolds' biocompatibility was checked by *in vitro* tests, including cell proliferation, cell morphology, and cell attachment in the C2C12 cell line. The CCS, CCS-SeNPs, CCS-SA-SeNPs, and CCS-PET-SeNPs scaffolds were washed with sterile PBS containing 500 U/mL penicillin and 500 µg/mL streptomycin, then sterilized at 121 °C for 20 min. The C2C12 cell line, sourced from the NCCS (Pune, India), was cultured in DMEM supplemented with 10 % fetal bovine serum, 100 U/mL penicillin, and 100 µg/mL streptomycin. Cells were maintained at 37 °C in a 5 % CO_2 environment with ~ 95 % humidity. Before the experiment, cells were trypsinized and re-suspended in DMEM with 10 % FBS, 100 U/mL penicillin, and 100 µg/mL streptomycin. A 15 µL aliquot of the cell suspension (4.2×10^{-5} cells/mL) was added to each scaffold and incubated at 37 °C for 48 hrs (Naveenkumar et al., 2023).

2.6. Propidium iodide (PI) staining

The scaffolds containing C2C12 cells, namely the CCS, CCS-SeNPs, CCS-SA-SeNPs and CCS-PET-SeNPs scaffolds, were fixed using a 3 % paraformaldehyde solution and incubated for 20 min. Following incubation, the scaffolds were thoroughly washed with ice-cold PBS (phosphate-buffered saline) at pH 7.5. Subsequently, the fixed scaffolds were stained with a solution of 50 mg/L propidium iodide (PI) for 20 min. After the staining process, the excess staining solution was removed using methanol (Naveenkumar et al., 2023).

2.7. Statistical analysis

All statistical analyses and calculations were conducted using Microsoft Office Excel 2021 and $p<0.0001$ was considered to indicate highly significant differences.

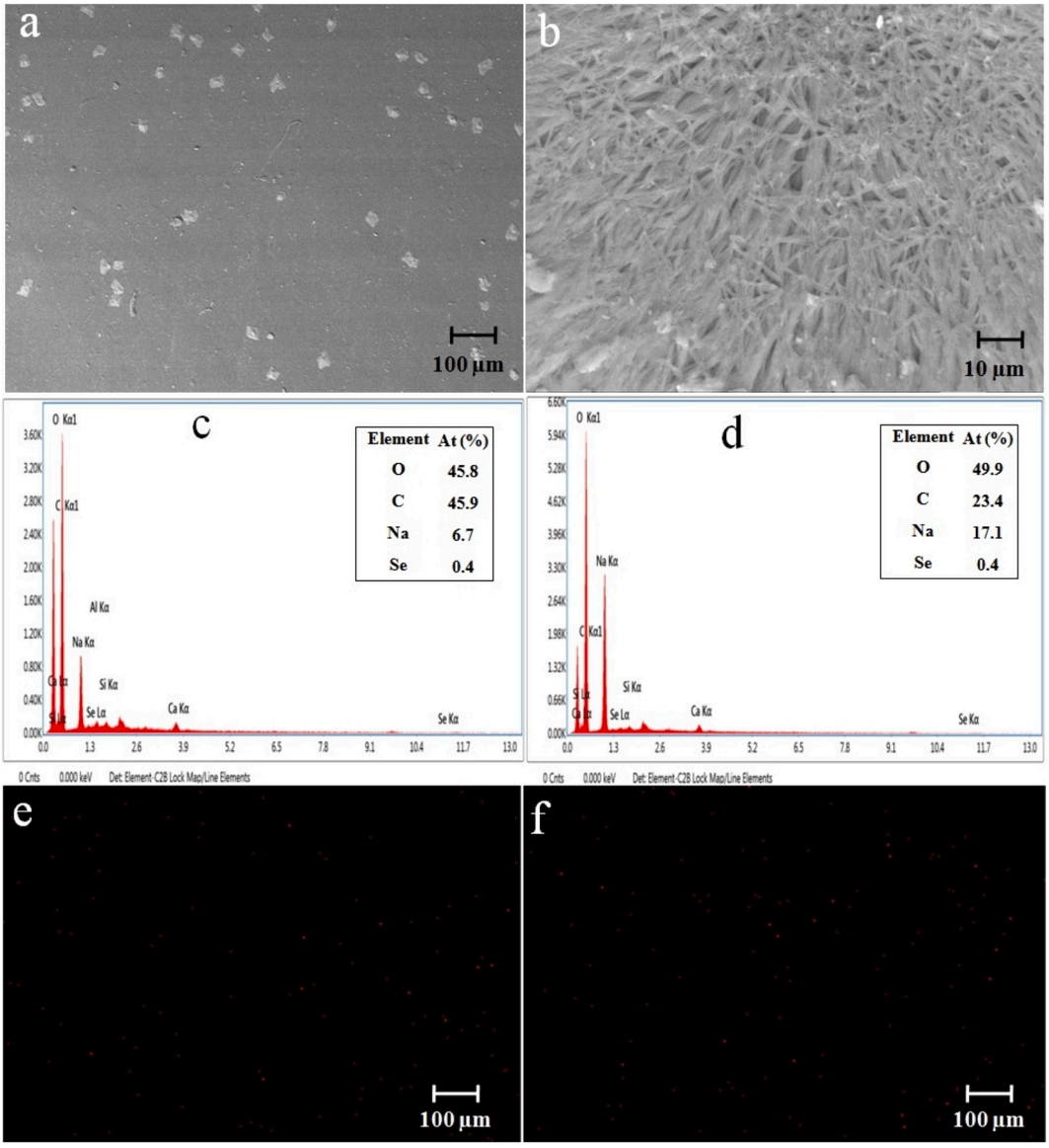

Fig. 3. (a-b) SEM observation of CCS-SA-SeNPs and CCS-PET-SeNPs scaffolds; (c) EDX spectrum and (e) EDX mapping of CCS-SA-SeNPs scaffold; (d) EDX spectrum and (f) EDX mapping of CCS-PET-SeNPs scaffold.

Table 1
Mechanical properties of CCS, CCS-SeNPs, CCS-SA-SeNPs and CCS-PET-SeNPs Scaffolds.

Scaffold	Tensile strength (N)
CCS	5.15
CCS-SeNPs	4.77
CCS-SA-SeNPs	4.05
CCS-PET-SeNPs	4.01

3. Results and discussion

3.1. XRD analysis

The XRD results of CCS, CCS-SeNPs, CCS-SA-SeNPs, and CCS-PET-SeNPs scaffolds are shown in Fig. 1. The observed XRD patterns display broad and indistinct peaks, indicative of a semi-crystalline nature within these scaffolds. The results showed a slight deviation from previous works in the XRD of Chitosan SeNPs film (Kalishwaralal et al., 2018). This phenomenon suggests that the synthesized materials combine crystalline and amorphous phases (Combes and Rey, 2010; Shah et al., 2006). The broadening of peaks may arise from various factors, such as polymorphic structures, varying crystallite sizes, or disordered regions within the materials (Vippagunta et al., 2001). The semi-crystalline nature of these scaffolds can be attributed to the specific synthesis conditions and the inherent properties of the constituent materials. The incorporation of selenium nanoparticles into the CCS and its combination with nanoparticles and polyethylene terephthalate likely influences the crystallinity of the overall structure (Uskoković et al., 2022). The amorphous regions could result from the interaction between the different components, leading to a heterogeneous structure with varying degrees of order. Understanding the semi-crystalline nature of the synthesized scaffolds is crucial for tailoring their properties for specific applications (Armentano et al., 2010; Dorozhkin, 2021). The observed XRD patterns provide valuable insights into the structural characteristics of these materials, laying the foundation for further exploration and optimization in the field of nanomaterial-based scaffolds.

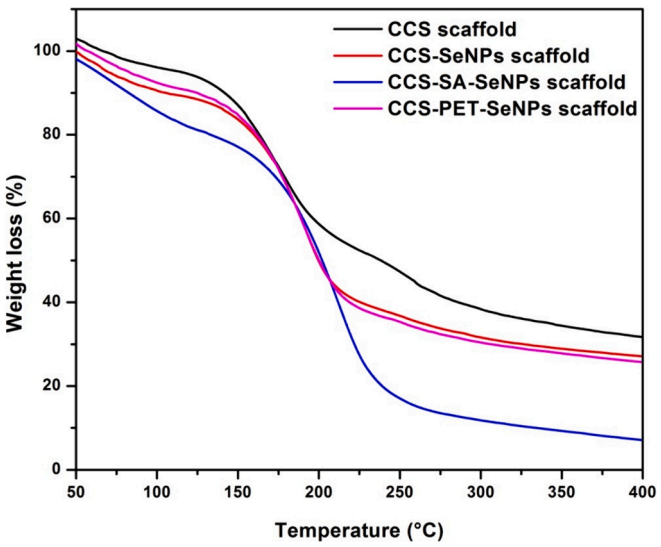

Fig. 4. Thermogravimetry (TG) curves illustrate the thermal behavior and decomposition of CCS scaffold, CCS-SeNPs scaffold, CCS-SA-SeNPs scaffold, and CCS-PET-SeNPs scaffolds.

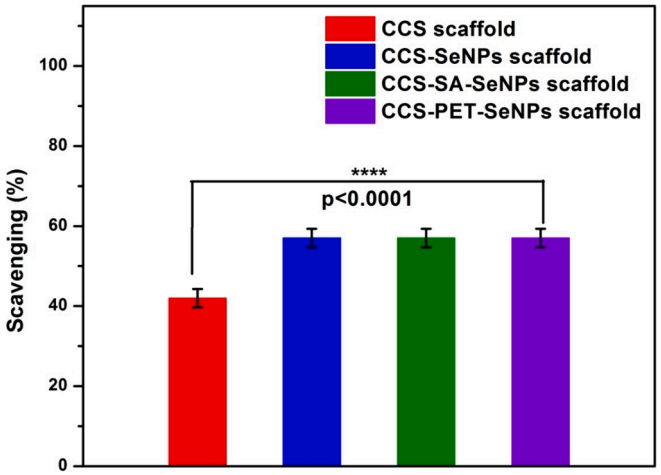

Fig. 5. Antioxidant study of CCS scaffold, CCS-SeNPs scaffold, CCS-SA-SeNPs scaffold and CCS-PET-SeNPs scaffold.

3.2. SEM-EDX studies

The SEM analysis examined the morphology of the CCS, CCS-SeNPs, CCS-SA-SeNPs and CCS-PET-SeNPs scaffolds. The results showed that the CCS and CCS-SA-SeNPs scaffolds exhibit solid-walled metrics and a smooth surface, as shown in Fig. 2(a) and 3(a). The present study's results deviated from those of other studies with scaffolds (Kalishwaralal et al., 2018). The CCS-SeNPs scaffold is also rod-shaped, as depicted in Fig. 2(b). At the same time, the CCS-PET-SeNPs scaffold is cross-linked and also rod-shaped, as illustrated in Fig. 3(b). Furthermore, the Energy-Dispersed X-ray (EDX) analysis was executed to determine the elemental composition of the scaffolds. The EDX analysis revealed that the main components of the CCS scaffold were carbon (C), oxygen (O), and sodium (Na), with no detectable selenium (Se) present. However, the addition of SeNPs, SA-SeNPs and PET-SeNPs, as shown in Fig. 2(b) and Fig. 3(a-b), resulted in the appearance of Se, which constituted 0.5 %, 0.4 % and 0.4 % atomic weight of the total components, respectively. This confirmed the successful incorporation of SeNPs into the scaffolds. The EDX mapping band confirmed that the SeNPs were uniformly distributed throughout the CCS-SeNPs, CCS-SA-SeNPs and CCS-PET-SeNPs scaffolds, as shown in Fig. 2(b) & Fig. 3(a-b). The uniform distribution of SeNPs is crucial for the potential applications of the scaffolds in biomedical fields, where a uniform distribution of nanoparticles is desirable (Nayak et al., 2021; Stevanović et al., 2015). Another study (Naveenkumar et al., 2023) confirmed through the EDX mapping spectrum that selenium nanoparticles were uniformly distributed throughout the AP-SeNPs scaffold.

3.3. Tensile strength

The results of the tensile strength of CCS, CCS-SeNPs, CCS-SA-SeNPs, and CCS-PET-SeNPs scaffolds are summarized in Table 1. In the current study, the tensile strength of the CCS scaffold was found to be 5.15 N. In comparison, the CCS-SeNPs scaffold exhibited a tensile strength of 4.77 N, the CCS-SA-SeNPs scaffold exhibited a tensile strength of 4.05 N and the CCS-PET-SeNPs scaffold exhibited a tensile strength of 4.01 N. The results showed slight deviations from those recently reported for the alginate-pectin-SeNPs scaffold (Naveenkumar et al., 2023). These findings confirmed a direct relationship between the nanoparticle concentrations and increased scaffold strength. As the concentration of magnetite nanoparticles in the PCL nanofibers increased, the tensile strength of the scaffold also increased (Rezaei et al., 2021). These findings revealed that incorporating $CaCO_3$ in chitosan/PVA nanofibers increased tensile strength and improved biocompatibility. Specifically, these enhancements were observed when the concentration of $CaCO_3$ varied within the range of 1 to 5 wt% (Hasan et al., 2018). Matching the mechanical properties of the biomaterial film with native cardiomyocytes also facilitates optimal cell attachment, proliferation, and differentiation, which can lead to improved tissue formation and regeneration. Ultimately, matching the mechanical properties of the biomaterial film to those of native cardiomyocytes can enhance the success of cardiac cell implantation and support tissue regeneration, thereby providing a promising avenue for developing effective cardiac therapies (Kalishwaralal et al., 2018). Overall, the evaluation of mechanical properties suggests that the CCS scaffolds have stronger tensile strength than the CCS-SeNPs, CCS-SA-SeNPs and CCS-PET-SeNPs scaffolds. The nanoparticles enhance the interfacial interaction between the scaffold matrix and themselves. This enhanced interaction improves stress transfer and more efficient load distribution, significantly increasing tensile strength (Hasan et al., 2018). However, it is essential to note that the nanoparticles may exhibit a weaker chemical or physical interaction with the scaffold material in some instances. This weaker interface can potentially limit the efficient stress transfer between the nanoparticles and the matrix, thereby causing a decrease in tensile strength (Domingues et al., 2014; Zare, 2016).

3.4. TGA measurements

Fig. 4 illustrates the TGA curves of CCS, CCS-SeNPs, CCS-SA-SeNPs, and CCS-PET-SeNPs scaffolds. All the scaffolds have shown better stability, up to 160 °C, with the maximum decomposition noted at 250 °C. A 100 % weight loss was noted at 400 °C. Specifically, the CCS scaffold exhibited a ~ 31 % weight loss, the CCS-SeNPs scaffold showed a ~ 27 % weight loss, the CCS-SAT-SeNPs scaffold displayed a 100 % weight loss, and the CCS-PET-SeNPs scaffold experienced a ~ 25 % weight loss. The CCS scaffold incorporated with SeNPs showed earlier degradation when compared with the CCS scaffold. The observation that the CCS scaffold, when integrated with SeNPs, undergoes earlier degradation than the pristine CCS scaffold is noteworthy. The results showed slight deviations from those previously reported for SeNPs-chitosan films (Kalishwaralal et al., 2018). This suggests that introducing selenium nanoparticles accelerates the thermal decomposition, possibly due to interactions between the CCS and the nanoparticles. These TGA results provide valuable information for designing and utilizing these scaffolds in applications where thermal stability is critical (Jain et al., 2020; Żółtowska et al., 2021). The differences in weight loss among the various

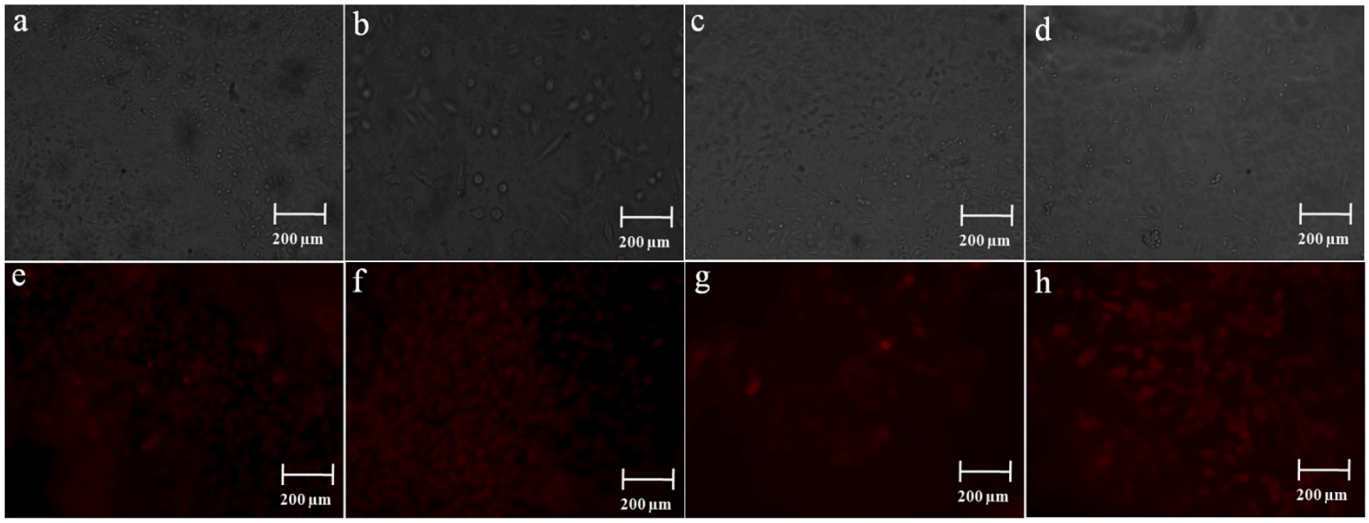

Fig. 6. Phase contrast microscopy images of (a-d) CCS, CCS-SeNPs, CCS-SA-SeNPs and CCS-PET scaffolds with C2C12 cells at 5th day; (e-h) PI stained with DNA condensation observed by CCS, CCS-SeNPs, CCS-SA-SeNPs and CCS-PET scaffolds with C2C12 cells on the 5th day.

Table 2
Various scaffolds used in cardiac tissue engineering.

Scaffold material	Type of cell	Result	Reference
Chitosan-carbon scaffold	Rat cardiomyocyte	Carbon nanofibers into chitosan-based scaffolds significantly enhanced the electrical conductivity and mechanical properties, fostering improved cellular activity and cardiac-specific gene expression. These findings suggest that chitosan/carbon nanofiber composites hold great promise for developing effective cardiac tissue constructs.	(Martins et al., 2014)
Polypyrrole (PPy)-chitosan hydrogel	Rat cardiomyocyte	Enhanced biocompatibility in rat cardiomyocyte	(Mihic et al., 2015)
Chitosan-Selenium nanoparticles film	H9C2	Chitosan- Selenium nanoparticles film showed good biocompatibility.	(Kalishwaralal et al., 2018)
Alginat-pectin-SeNPs scaffold	C2C12	Alginat-pectin-SeNPs scaffold highlighted, making them suitable substrates for cell growth and biocompatibility.	(Naveenkumar et al., 2023)

scaffolds highlight the influence of nanoparticle incorporation on thermal behavior, offering avenues for further optimization and fine-tuning of these materials for specific applications (Bekas et al., 2019; Konwarh et al., 2013).

3.5. Antioxidant activity

The scavenging ability of CCS-SeNPs, CCS-SA-SeNPs, and CCS-PET-SeNPs scaffolds on DPPH was stronger than that of the CCS scaffold. Specifically, no significant changes were observed in the scavenging activity of CCS-SeNPs, CCS-SA-SeNPs, and CCS-PET-SeNPs scaffolds, which exhibited scavenging activities of 57 % each. This is notably higher than the 42 % scavenging activity observed for the CCS scaffold, as depicted in Fig. 5. The obtained results showed slight deviations from those of other previously reported scaffolds, with alginate-pectin and alginate-pectin-SeNPs scaffolds exhibiting antioxidant activities of ~ 41.02 % and ~ 61.52 %, respectively (Naveenkumar et al., 2023). The enhanced scavenging ability observed in the selenium nanoparticle-loaded scaffolds (CCS-SeNPs, CCS-SA-SeNPs, and CCS-PET-SeNPs) suggests a synergistic effect between selenium nanoparticles. Selenium is well-known for its antioxidant properties, and its combination with CCS amplifies the scavenging capacity. The lack of significant differences among these selenium-loaded scaffolds indicates a consistent and strong antioxidant performance across different compositions (Hou et al., 2021).

3.6. Morphology of C2C12 cell line in scaffolds

In Fig. 6 (a-d) display the morphological characteristics of C2C12 cells attached to scaffolds, including CCS, CCS-SeNPs, CCS-SA-SeNPs, and CCS-PET-SeNPs. These cell images were captured in fluorescence microscopy (EVOS epifluorescence microscope). The C2C12 cells were cultivated on CCS, CCS-SeNPs, CCS-SA-SeNPs, and CCS-PET-SeNPs scaffolds to illustrate their attachment and morphology. A notable contrast in cell density was observed between the CCS scaffold and the CCS-SeNPs, CCS-SA-SeNPs, and CCS-PET-SeNPs scaffolds. This observation suggests that C2C12 cells exhibit enhanced proliferation when cultured on CCS-SeNPs, CCS-SA-SeNPs, and CCS-PET-SeNPs scaffolds. These C2C12 cells exhibited a spindle-shaped morphology, and this characteristic remained consistent even after 5 days of culture. Naveenkumar et al., 2023 reported the growth of C2C12 cells on both AP and AP-SeNPs scaffolds to evaluate cell morphology and attachment. They noted significant differences in cell density, indicating enhanced proliferation of C2C12 cells on the AP-SeNPs scaffold compared to the AP scaffold. Another study (Ricotti et al., 2012) reported that the surfaces of polystyrene and polyhydroxybutyrate (PHB) film led to an increased fusion index in C2C12 and H9C2 cell lines when cultured on nanofibrous (nF) substrates. This increase was particularly prominent in aligned nF samples, which remained distinct from other substrates after 3 days of differentiation. For C2C12 cells, no significant differences in myotube length were observed even after 3 days of differentiation across different sample types. In terms of scaffold surface characteristics, it is worth noting that smooth surfaces of scaffolds often induce strong inflammatory reactions, potentially leading to the formation of a fibrotic capsule around the implant. The results indicated that C2C12 cells

exhibited more efficient proliferation when cultured on the CCS-SeNPs, CCS-SA-SeNPs and CCS-PET-SeNPs scaffold compared to the CCS scaffold. These findings suggest that the smooth surfaces of the CCS-SeNPs and CCS-PET-SeNPs scaffolds promote enhanced cell attachment and proliferation, which may ultimately contribute to improved tissue regeneration. The scaffold materials and their effects on cellular behavior, for advancing cardiac tissue engineering as shown in Table 2.

3.7. Evaluation of nucleus morphology using PI staining

The C2C12 cells in various scaffolds, including CCS, CCS-SeNPs, CCS-SA-SeNPs, and CCS-PET-SeNPs, were stained PI to observe nucleus morphology. The nuclei in all these cells appeared circular, and there were no noteworthy variances compared to the control CCS scaffold, as depicted in Fig. 6 (e-h). This observation is consistent with the findings in a study by Kalishwaralal et al. (Kalishwaralal et al., 2018), where chitosan-SeNPs and chitosan films were used to stain H9C2 cells with propidium iodide. In that study, the nucleus of H9C2 cells exhibited a circular and structurally intact appearance, regardless of the type of film used. The study concluded that incorporating different sizes of SeNPs into chitosan films did not lead to noticeable changes in ROS production or alterations in nuclear structure in H9C2 cells after 5 days of culture.

4. Conclusion

In conclusion, this study successfully developed scaffolds with enhanced mechanical strength, thermal stability, and antioxidant properties to improve cell attachment and proliferation, particularly for the C2C12 cell line, a model for muscle cells, including cardiac muscle. Incorporating SA-SeNPs and PET-SeNPs into chitosan-collagen scaffolds significantly improved their functional properties without severely compromising mechanical strength. Antioxidant activity tests highlighted enhanced scavenging capabilities in SeNPs-loaded scaffolds. Morphological studies of C2C12 cells cultured on these scaffolds indicated improved proliferation on SeNPs-enhanced scaffolds. Nucleus morphology assessments showed no significant alterations, suggesting that SeNPs do not adversely affect cellular structure. These findings suggest that such scaffolds have promising applications in cardiac tissue engineering, potentially supporting tissue regeneration and repair by providing a conducive environment for cell growth and reducing oxidative stress. Future work could involve *in vivo* studies to evaluate these scaffolds' long-term biocompatibility and functional performance in cardiac tissue repair. Additionally, exploring the incorporation of other bioactive nanoparticles or growth factors may further enhance these scaffolds' regenerative capabilities and clinical potential.

CRediT authorship contribution statement

Suresh Naveenkumar: Formal analysis, Methodology, Project administration, Resources, Validation, Writing – original draft. **Johnson Retnaraj Samuel Selvan Christyraj:** Data curation, Resources, Validation, Visualization. **K. Kaviyarasu:** Formal analysis, Funding acquisition, Resources, Validation, Visualization. **Azhaguchamy Muthukumaran:** Conceptualization, Funding acquisition, Investigation, Methodology, Supervision, Validation, Visualization.

Declaration of competing interest

The authors declare that they have no known competing financial interests or personal relationships that could have appeared to influence the work reported in this paper.

Acknowledgment

In this paper, we acknowledge the support for the project provided by the Indian Council of Medical Research (ICMR), Government of India (GOI) (35/12/2020-Nano/BMS). Thank you to Mr. Krishna Prabhu at KARE's International Research Center (IRC) for offering assistance with FTIR and XRD analysis.

References

(NIH), U.S.D. of H.& H.S. the O. of D.S. (ODS) of the N.I. of H., 2019. Selenium Fact Sheet for Health Professionals. NIH Office 320.

Armentano, I., Dottori, M., Fortunati, E., Mattioli, S., Kenny, J.M., 2010. Biodegradable polymer matrix nanocomposites for tissue engineering: A review. Polym. Degrad. Stab. 95, 2126–2146. https://doi.org/10.1016/j.polymdegradstab.2010.06.007.

Bekas, D.G., Hou, Y., Liu, Y., Panesar, A., 2019. 3D printing to enable multifunctionality in polymer-based composites: A review. Compos. B Eng. 179, 107540 https://doi.org/10.1016/j.compositesb.2019.107540.

Chan, B.P., Leong, K.W., 2008. Scaffolding in tissue engineering: general approaches and tissue-specific considerations. European Spine Journal : Official Publication of the European Spine Society, the European Spinal Deformity Society, and the European Section of the Cervical Spine Research Society 17 (Suppl 4), 467–479. https://doi.org/10.1007/s00586-008-0745-3.

Combes, C., Rey, C., 2010. Amorphous calcium phosphates: Synthesis, properties and uses in biomaterials. Acta Biomater. 6, 3362–3378. https://doi.org/10.1016/j.actbio.2010.02.017.

Domingues, R.M.A., Gomes, M.E., Reis, R.L., 2014. The Potential of Cellulose Nanocrystals in Tissue Engineering Strategies. Biomacromolecules 15, 2327–2346. https://doi.org/10.1021/bm500524s.

Dorozhkin, S.V., 2021. Synthetic amorphous calcium phosphates (ACPs): preparation, structure, properties, and biomedical applications. Biomater. Sci. 9, 7748–7798. https://doi.org/10.1039/D1BM01239H.

Erkekoğlu, P., Rachidi, W., De Rosa, V., Giray, B., Favier, A., Hıncal, F., 2010. Protective effect of selenium supplementation on the genotoxicity of di(2-ethylhexyl)phthalate and mono(2-ethylhexyl)phthalate treatment in LNCaP cells. Free Radic. Biol. Med. 49, 559–566. https://doi.org/10.1016/j.freeradbiomed.2010.04.038.

Han, F., Meng, Q., Xie, E., Li, K., Hu, J., Chen, Q., Li, J., Han, F., 2023. Engineered biomimetic micro/nanomaterials for tissue regeneration. Frontiers in Bioengineering and. Biotechnology.

Hasan, A., Morshed, M., Memic, A., Hassan, S., Webster, T.J., Marei, H.-E.-S., 2018. Nanoparticles in tissue engineering: applications, challenges and prospects. Int. J. Nanomed. 13, 5637–5655. https://doi.org/10.2147/IJN.S153758.

Hou, Y., Wang, W., Bartolo, P., 2021. A concise review on the role of selenium for bone cancer applications. Bone 149, 115974. https://doi.org/10.1016/j.bone.2021.115974.

Islam, M.M., Shahruzzaman, M., Biswas, S., Nurus Sakib, M., Rashid, T.U., 2020. Chitosan based bioactive materials in tissue engineering applications-a review. Bioact. Mater. 5, 164–183. https://doi.org/10.1016/j.bioactmat.2020.01.012.

Jain, S., Fuoco, T., Yassin, M.A., Mustafa, K., Finne-Wistrand, A., 2020. Printability and critical insight into polymer properties during direct-extrusion based 3D printing of medical grade polylactide and copolyesters. Biomacromolecules 21, 388–396. https://doi.org/10.1021/acs.biomac.9b01112.

Kalishwaralal, K., Jeyabharathi, S., Sundar, K., Selvamani, S., Prasanna, M., Muthukumaran, A., 2018. A novel biocompatible chitosan–Selenium nanoparticles (SeNPs) film with electrical conductivity for cardiac tissue engineering application. Mater. Sci. Eng. C 92, 151–160. https://doi.org/10.1016/j.msec.2018.06.036.

Karthick Raja Namasivayam, S., Nizar, M., Samrat, K., Sudarsan, A. V, Valli Nachiyar, C., Arvind Bharani, R.S., 2022. Green Synthesis of Chitosan–Selenium Bionanocomposite with High Biocompatibility and Its Marked Impact on Las B and RhII Genes Expression in Pseudomonas aeruginosa. J. Inorg. Organometall. Polym. Mater. 32, 4186–4203. doi: 10.1007/s10904-022-02431-9.

Konwarh, R., Karak, N., Misra, M., 2013. Electrospun cellulose acetate nanofibers: The present status and gamut of biotechnological applications. Biotechnol. Adv. 31, 421–437. https://doi.org/10.1016/j.biotechadv.2013.01.002.

Lei, L., Mu, J., Zheng, Y., Liu, Y., 2023. Selenium Deficiency-Induced Oxidative Stress Causes Myocardial Injury in Calves by Activating Inflammation, Apoptosis, and Necroptosis. Antioxidants. https://doi.org/10.3390/antiox12020229.

Li, Y., Liu, Y., Li, R., Bai, H., Zhu, Z., Zhu, L., Zhu, C., Che, Z., Liu, H., Wang, J., Huang, L., 2021. Collagen-based biomaterials for bone tissue engineering. Mater. Des. 210, 110049 https://doi.org/10.1016/j.matdes.2021.110049.

Martins, A.M., Eng, G., Caridade, S.G., Mano, J.F., Reis, R.L., Vunjak-Novakovic, G., 2014. Electrically Conductive Chitosan/Carbon Scaffolds for Cardiac Tissue Engineering. Biomacromolecules 15, 635–643. https://doi.org/10.1021/bm401679q.

Mihic, A., Cui, Z., Wu, J., Vlacic, G., Miyagi, Y., Li, S.-H., Lu, S., Sung, H.-W., Weisel, R. D., Li, R.-K., 2015. A conductive polymer hydrogel supports cell electrical signaling and improves cardiac function after implantation into myocardial infarct. Circulation 132, 772–784.

Namasivayam, S.K.R., Vigneshwaraprakash, L., Samrat, K., Kavisri, M., Moovendhan, M., Bharani, R.S.A., 2023. Enhanced Antibacterial Activity of Highly Biocompatible Polymeric Core-Shell Levofloxacin Gold Nanocomposite Formulation Against Pseudomonas aeruginosa. Appl. Biochem. Biotechnol. 195, 1837–1861. https://doi.org/10.1007/s12010-022-04256-1.

Naveenkumar, S., Venkateshan, N., Kaviyarasu, K., Christyraj, J.R.S.S., Muthukumaran, A., 2023. Optimum performance of a novel biocompatible scaffold comprising alginate-pectin-selenium nanoparticles for cardiac tissue engineering using C2C12 cells. J. Mol. Struct. 1294, 136457 https://doi.org/10.1016/j.molstruc.2023.136457.

Naveenkumar, S., Alagumanikumaran, N., Kaviyarasu, K., Muthukumaran, A., 2024. Influence of encapsulated sodium alginates and pectin on selenium nanoparticles and efficient cardioprotective effect in C2C12 cell line. J. Nanopart. Res. 26, 52. https://doi.org/10.1007/s11051-024-05956-x.

Naveenkumar, S., Venkateshan, N., Muthukumaran, A., 2022. Selenium Nanoparticles: Treatments in Tissue Engineering for Alcoholic Cardiomyopathy BT - Nanomaterials for Energy Conversion, Biomedical and Environmental Applications, in: Kasinathan, K., Elshikh, M.S., Al Farraj, D.A.-A. (Eds.), . Springer Nature Singapore, Singapore, pp. 235–253. doi: 10.1007/978-981-19-2639-6_10.

Nayak, V., Singh, K.R.B., Singh, A.K., Singh, R.P., 2021. Potentialities of selenium nanoparticles in biomedical science. New J. Chem. 45, 2849–2878. https://doi.org/10.1039/D0NJ05884J.

Ramoutar, R.R., Brumaghim, J.L., 2010. Antioxidant and anticancer properties and mechanisms of inorganic selenium, oxo-sulfur, and oxo-selenium compounds. Cell Biochem. Biophys. 58, 1–23. https://doi.org/10.1007/s12013-010-9088-x.

Reddy, M.S., Ponnamma, D., Choudhary, R., Sadasivuni, K.K., 2021. A comparative review of natural and synthetic biopolymer composite scaffolds. Polymers. https://doi.org/10.3390/polym13071105.

Rezaei, V., Mirzaei, E., Taghizadeh, S.-M., Berenjian, A., Ebrahiminezhad, A., 2021. Nano iron oxide-PCL composite as an improved soft tissue scaffold. Processes. https://doi.org/10.3390/pr9091559.

Ricotti, L., Polini, A., Genchi, G.G., Ciofani, G., Iandolo, D., Vazão, H., Mattoli, V., Ferreira, L., Menciassi, A., Pisignano, D., 2012. Proliferation and skeletal myotube formation capability of C2C12 and H9c2 cells on isotropic and anisotropic electrospun nanofibrous PHB scaffolds. Biomed. Mater. 7, 35010. https://doi.org/10.1088/1748-6041/7/3/035010.

Shah, B., Kakumanu, V.K., Bansal, A.K., 2006. Analytical techniques for quantification of amorphous/crystalline phases in pharmaceutical solids. J. Pharm. Sci. 95, 1641–1665. https://doi.org/10.1002/jps.20644.

Sidhu, M., Sharma, M., Bhatia, M., Awasthi, Y.C., Nath, R., 1993. Effect of chronic cadmium exposure on glutathione S-transferase and glutathione peroxidase activities in Rhesus monkey: the role of selenium. Toxicology 83, 203–213. https://doi.org/10.1016/0300-483X(93)90102-X.

Sowmya, R., Namasivayam, K.R., Krithika Shree, S., 2024. A critical review on nano-selenium based materials: synthesis, biomedicine applications and biocompatibility assessment. J. Inorg. Organomet. Polym Mater. https://doi.org/10.1007/s10904-023-02959-4.

Stevanović, M., Filipović, N., Djurdjević, J., Lukić, M., Milenković, M., Boccaccini, A., 2015. 45S5Bioglass®-based scaffolds coated with selenium nanoparticles or with poly(lactide-co-glycolide)/selenium particles: processing, evaluation and antibacterial activity. Colloids Surf. B Biointerf. 132, 208–215. https://doi.org/10.1016/j.colsurfb.2015.05.024.

Uskoković, V., Pejčić, A., Koliqi, R., Anđelković, Z., 2022. Polymeric nanotechnologies for the treatment of periodontitis: a chronological review. Int. J. Pharm. 625, 122065 https://doi.org/10.1016/j.ijpharm.2022.122065.

Vippagunta, S.R., Brittain, H.G., Grant, D.J.W., 2001. Crystalline solids. Adv. Drug Deliv. Rev. 48, 3–26. https://doi.org/10.1016/S0169-409X(01)00097-7.

Zare, Y., 2016. A model for tensile strength of polymer/clay nanocomposites assuming complete and incomplete interfacial adhesion between the polymer matrix and nanoparticles by the average normal stress in clay platelets. RSC Adv. 6, 57969–57976. https://doi.org/10.1039/C6RA04132A.

Zheng, X., Zhang, P., Fu, Z., Meng, S., Dai, L., Yang, H., 2021. Applications of nanomaterials in tissue engineering. RSC Adv. 11, 19041–19058.

Żółtowska, S., Koltsov, I., Alejski, K., Ehrlich, H., Ciałkowski, M., Jesionowski, T., 2021. Thermal decomposition behaviour and numerical fitting for the pyrolysis kinetics of 3D spongin-based scaffolds. the classic approach. Polym. Test. 97, 107148 https://doi.org/10.1016/j.polymertesting.2021.107148.